DOI: 10.21062/mft.2025.022 http://www.journalmt.com

SEM Analysis of Surface Layers with Variable Ra Parameters for Tribological Optimization in Design Engineering

Paweł Knast (0000-0001-7430-9914)[1], Jana Petrů (0000-0002-2378-5678)[2], Stanislaw Legutko (0000-0001-8973-5035)[3], Lubomir Soos (0000-0003-3161-5609)[4], Marcela Pokusova (0000-0002-1525-2521)[4]
[1]Polytechnic Faculty, Calisia University, 4 Nowy Świat street, 62-800 Kalisz, Poland; p.knast@uniwersytetkaliski.edu.pl
[2]Faculty of Mechanical Engineering, Department of Machining, Assembly and Engineering Metrology, VSB - Technical University of Ostrava, 70 800 Ostrava, Czech Republic; jana.petru@vsb.cz
[3]Faculty of Mechanical Engineering, Poznan University of Technology, 3 Piotrowo street, 60-965 Poznan, Poland; stanislaw.legutko@put.poznan.pl
[4]Faculty of Mechanical Engineering, Slovak Technical University, Námestie slobody 17, 812 31 Bratislava 1, Slovak Republic; lubomir.soos@stuba.sk; marcela.pokusova@stuba.sk

In this study, the microstructure of surface layers with varying roughness (Ra parameters) was analysed using scanning electron microscopy (SEM) to optimize tribological properties in engineering design. SEM revealed key microstructural features – sharp and mild protrusions, pitting, microcracks and contaminants – that were not available in traditional profilometry. Reducing the Ra value improved surface uniformity by reducing irregularities and defect lengths, which had a positive effect on tribological properties and surface durability. However, defects were still present even at Ra < 1.25 μm, indicating the "Law of Microstructural Roughness," which emphasizes the inevitability of surface irregularities despite minimizing roughness. The integration of SEM results with profilometric methods enabled comprehensive identification and assessment of defects, combining microstructure with tribological properties. Results suggest that controlled roughness is key in combining materials and optimizing functional surfaces, particularly in the aerospace, biomedical and automotive industries, where reliability under demanding operating conditions is a priority.

Keywords: Tribology, Surface roughness, SEM analysis, Microstructural defects, Engineering design

1 Introduction

Surface roughness plays a crucial role in the performance and longevity of mechanical components, particularly in industries where precision and durability are paramount, such as aerospace, automotive, and biomedical engineering. The most used roughness parameter, arithmetic mean deviation (Ra), provides a general assessment of surface quality. However, Ra alone does not capture critical microstructural details such as pits, cracks, and irregularities, which significantly affect the tribological properties of surfaces [1–3].

Traditional roughness measurement methods, such as contact profilometry, offer reliable numerical values but fail to provide comprehensive microstructural insight [4,5]. In contrast, scanning electron microscopy (SEM) enables detailed surface characterization, revealing microstructural defects that influence wear resistance and friction performance [6,7]. Researchers have highlighted that integrating SEM with conventional roughness measurement techniques provides a more holistic view of surface characteristics [8,9].

Microstructural defects, including pitting, microcracks, and contaminations, can alter the functional properties of a material, affecting its frictional behaviour and durability. Nguyen et al. [10] and Li et al. [11] emphasized that even minor irregularities at the microstructural level can significantly influence wear mechanisms. Similarly, Abellán-Nebot et al. [3] demonstrated that machining parameters play a vital role in shaping the final surface microstructure, particularly in sustainable manufacturing contexts.

Advanced manufacturing methods, including additive manufacturing and laser processing, have shown significant potential in improving surface quality. Buj-Corral et al. [2] examined the effects of additive manufacturing parameters on surface roughness, while Szymański et al. [6] explored the impact of laser processing on hybrid metal matrix composites. Both studies confirmed that optimizing machining conditions is essential for achieving desirable surface properties. However, there remains a knowledge gap in understanding how SEM-detected microstructural variations correlate with Ra values and their implications for tribology.

To bridge this gap, the present study investigates the correlation between Ra values and microstructural defects identified through SEM analysis. Specifically, the study aims to address the following research questions in the three ranges presented below.

- What additional microstructural insights can be obtained through SEM compared to traditional profilometric methods?
- How do microstructural differences associated with varying Ra values influence tribological performance?
- Can integrating SEM with conventional roughness measurement techniques enhance the understanding of surface functionality?

A literature review suggests that surface irregularities persist even at lower Ra values, which may still impact material performance [12,13]. While reducing Ra improves uniformity, defects remain, as evidenced by studies on surface treatments and their effects on stress concentration and wear resistance [14].

By analysing surfaces with Ra values of 1.25 μm and 2.5 μm, obtained through milling and subsequently examined using SEM, this study aims to provide a comprehensive understanding of the relationship between roughness parameters and tribological properties. The findings will contribute to the optimization of machining processes, particularly in industries where precise surface control is critical.

2 Materials and Methods

The aim of the study was to compare the results of surface microstructure analysis obtained by scanning electron microscopy (SEM) with those obtained using traditional profilometric methods, such as a tactile profilometer. It was assumed that microscopic techniques could provide additional relevant information about the microstructure of the surface, which would allow for a better understanding of its functional properties.

The study was based on three key questions concerning the scope of additional information provided by SEM compared to profilometry, the impact of differences in microstructure resulting from the value of the Ra parameter on tribological properties, and the possibility of a comprehensive understanding of the relationship between microstructure and surface properties by integrating SEM results with classical measurement methods.

Two steel samples measuring 20 × 20 × 20 mm were prepared for analysis, processed on a DMG MORI DMU 50 CNC milling machine, whose spindle operates in the range of 20 to 10 000 rpm. The samples differed in the value of the mean arithmetic deviation of the Ra profile – the first had Ra = 1.25 μm, and the second Ra = 2.5 μm. This allowed for a detailed analysis of the effect of roughness on the surface microstructure, while ensuring precise control of the machining conditions and increasing the reliability of the results.

Cutting data has been selected in accordance with Sandvik Coromant recommendations for carbon structural steel with a hardness of 175 HB. The stock was 30 × 30 × 30 mm, and the layer of material was stripped in two passes, with the first strip being 4.6mm and the second being 0.4 mm. The key to achieving a roughness of Ra = 1.25 μm, the second pass was made at a cutting speed of 355 $m \cdot min^{-1}$ and a spindle speed of 6 030 rpm. The feed per blade was 0.127 mm, while the feed speed on the cutting diameter was 1 830 $mm \cdot min^{-1}$. For a specimen with Ra = 2.5 μm, a cutting speed of 358 $m \cdot min^{-1}$ was used at the same spindle speed, while the feed per tooth was increased to 0.152 mm, while the feed rate at the cutting diameter was 1 830 $mm \cdot min^{-1}$.

After the machining was completed, profilometric measurements were carried out using the Mitutoyo Surfest SJ-210 contact profilometer. This tool, widely used in industry, served as a reference for SEM results. The measurement results confirmed the compliance of the samples with the assumed Ra values, which was crucial for further analysis (Fig. 1).

Then, the samples were examined using a Hitachi SU3500 scanning electron microscope, available at the Poznan Science and Technology Park. SEM analysis allowed for detailed imaging of the surface microstructure and identification of features such as the number and shape of irregularities, the presence of pitting and the distribution of contaminants. Observations were made at magnifications ranging from 100× to 3000×, which enabled the analysis of both surface topography and detailed microstructural features. To ensure the reproducibility of the results, the microscope's constant operating parameters were used, including an accelerating voltage of 15 kV and an operating distance of 6.5 mm.

To allow quantitative comparison of the microstructure, the SEM images were divided into a grid of 43 columns and 34 rows, resulting in a total of 1462 squares for each image (Fig. 2 and Fig. 3). This division allowed for precise counting of surface deformations, including the number of sharp and benign protrusions, the width of cracks, and the number and distribution of pits. The presence and size of contaminants were also analysed, as well as the length and distribution of microcracks. The collected data were tabulated (Table 1–7), which enabled a systematic assessment of the influence of microstructure on surface properties.

SEM analysis provided answers to key research questions. It has been shown that the use of this method allows the identification of microstructural details that are not visible in traditional Ra

measurements. Thanks to the SEM technique, it was possible to observe pitting, sharp edges, structural irregularities and microcracks, which can affect the tribological properties of the surface. In addition, the comparison of samples with different Ra values showed that surfaces with lower roughness have a more homogeneous structure, fewer sharp edges and a more regular pitting arrangement, potentially improving their functional properties. Ultimately, the integration of SEM results with profilometric data enabled a comprehensive assessment of the surface microstructure. SEM provided detailed information on the shape and distribution of defects that were not visible in traditional profilometric measurements.

The presented research methodology was developed to better understand the influence of surface irregularities on its tribological properties. The results of the study have applications in the design of mechanical components, particularly in high-precision industries such as aerospace, and biomedical. The integration of SEM results with classic profilometric methods enables more precise control and optimization of surface treatment processes, which translates into improved durability and functionality of engineering components.

3 Results and Discussion

The conducted research enabled a detailed analysis of the microstructure of the surface layer of samples with different Ra roughness using profilometric techniques and scanning electron microscopy (SEM). The combination of these methods allowed for a comprehensive assessment of the surface, considering its topography and microstructure.

The surface roughness analysis was carried out using a profilometer. The results are presented in Fig. 1 in the form of graphs illustrating the differences in Ra parameters, amounting to an average of 1.25 μm and 2.5 μm. Although Ra measurements provided numerical values, this method did not allow for full visualization of surface features. This limited its usefulness in precise tribological analyses, especially in the context of the correlation of numerical parameters with real microstructural features.

Roughness plots showed that samples with a higher Ra value had greater amplitude variation, which may have affected their tribological properties. The Ra test itself, although commonly used by designers, does not provide information about the actual appearance of surface irregularities. Therefore, the aim of further research was to capture morphological parameters in detail using electron microscopy.

Different magnifications were used in the test procedure to determine at what magnification differences affecting roughness changes were visible. To estimate the number and magnitude of surface damage, the image area was divided into a grid of squares, as shown in Fig. 2 and Fig. 3a, where the classification and counting of defects defined in Fig. 3b was performed. To enable readers to make an independent, critical analysis, the subsequent illustrations do not include the overlay of the grid and damage descriptions. The number of surface deformations was so large that their direct marking could make it difficult for the reader to draw his own conclusions.

The first tests were carried out at x100 magnification (Fig. 4), which showed significant differences in the surface structure of the samples. Surfaces with higher roughness (Ra < 2.5) were characterized by numerous sharp edges, irregular distribution of vices and the presence of defects. In contrast, samples with a lower Ra value (Ra < 1.25) had a more homogeneous structure and fewer unevenness's. These results are summarized in detail in Table 1. However, the x100 magnification was not sufficient to accurately visualize subtle differences, such as the shape of micro-indentations or the detailed arrangement of defects. Therefore, the research was continued at higher magnifications.

Performing the analysis at magnifications of x500, x1000 and x1500 (Fig. 5, 6, 7) allowed for better capture of microstructural details, such as micro-pitting, structural irregularities and the presence of contaminants. A detailed comparison of the results can be found in Tabs. 2 and 3. It was found that lower Ra values were associated with a more regular surface geometry and fewer micro-pitting, which had a positive effect on tribological properties. On the other hand, surfaces with a higher Ra value were characterized by greater irregularity, which increased the risk of local stress concentrations.

Further studies at magnifications of x2000, x2500 and x3000 (Fig. 8, 9, 10) al-lowed to capture details such as the shape of micro-pits or the depth of defects. Tabs. 4 and 5 present data on the number of sharp edges, micro-pitting and contamination. The results clearly indicated that surfaces with a lower Ra value are characterized by greater uniformity, which can contribute to reducing friction and improving the durability of mechanical components.

The results obtained confirm the legitimacy of the integration of profilometric and SEM methods. The profilometer provides numerical values that are complemented by detailed microstructure analysis obtained with SEM. This approach allows for a more complete understanding of surface properties and the identification of features that may affect its functionality, such as stress concentrations or failure initiation.

The methodology is particularly important from the point of view of designing mechanical elements, where even minor defects can lead to material fatigue, corrosion and damage to a critical element of the designed structure. The integration of advanced imaging techniques and traditional measurement methods enables precise surface design with optimized tribological properties.

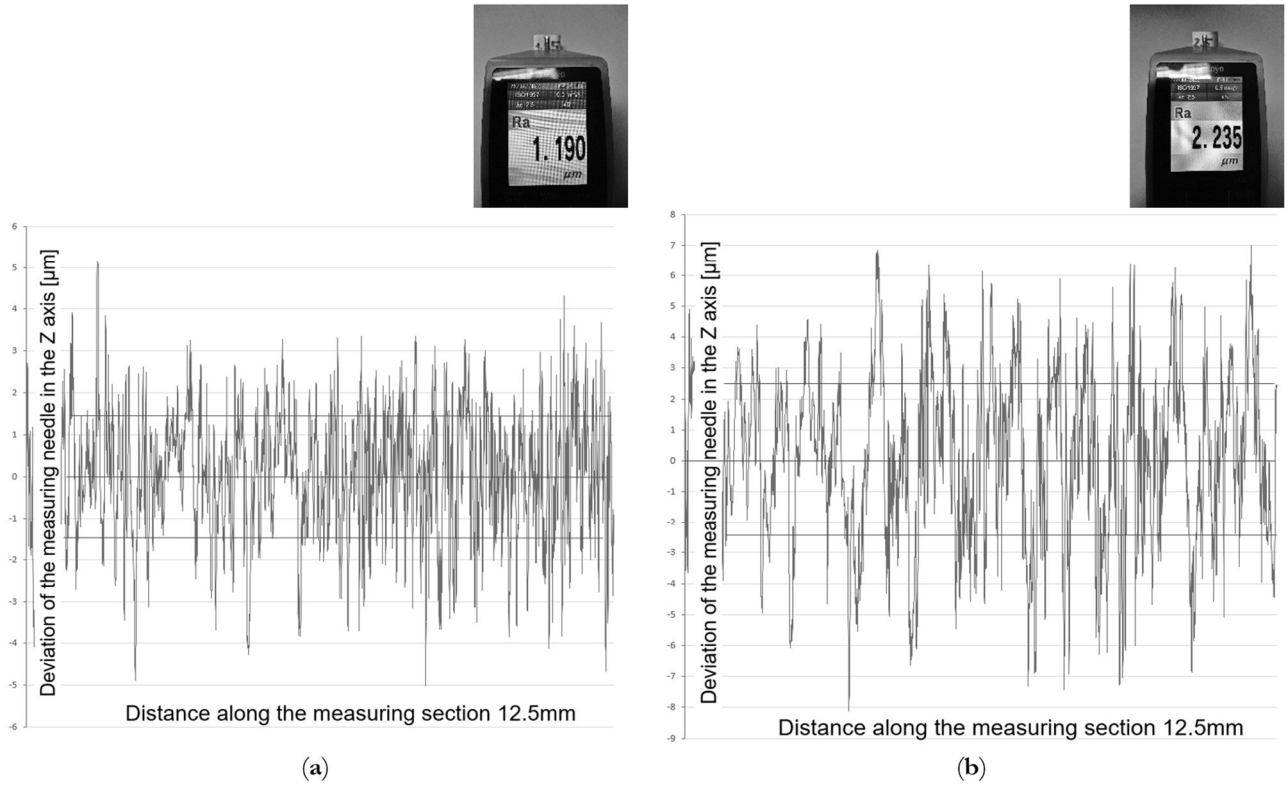

(**a**) (**b**)

Fig. 1 *Surface roughness diagrams for two cubic measuring samples (20 × 20 × 20 mm) processed on a DMG MORI milling machine; The roughness was measured along a selected section of 12.5 mm*

In the Fig. 1 (a) the diagram corresponds to the first sample, showing a roughness value of Ra = 1.190 µm. In the Fig. 1 (b) the diagram corresponds to the second sample, showing a roughness value of Ra = 2.255 µm.

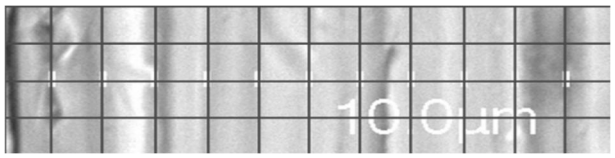

Fig. 2 *A grid with a division of 12x7 (84 squares) was applied to the SEM image, corresponding to the scale given in the lower right corner of the photo*

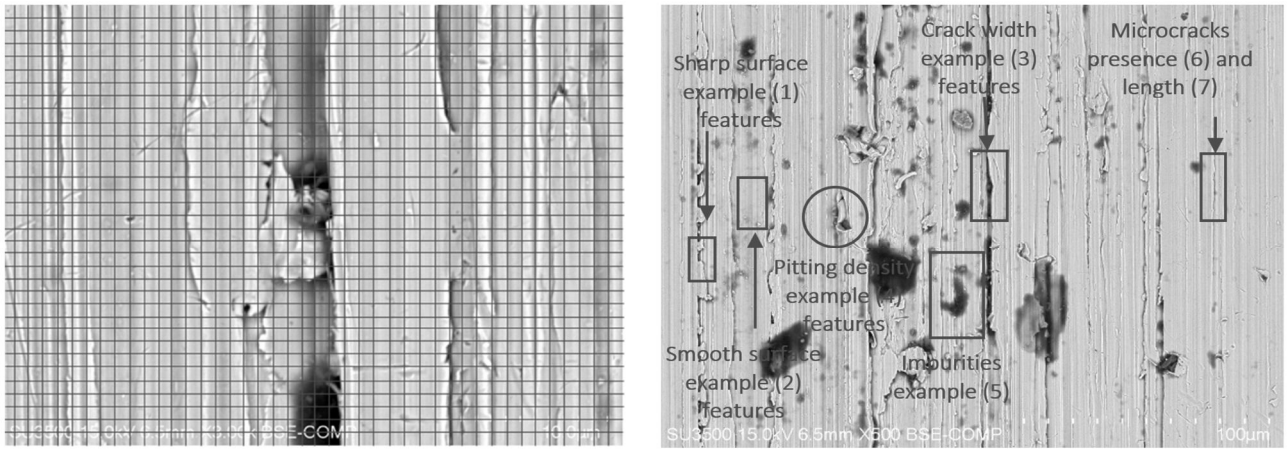

(**a**) (**b**)

Fig. 3 *SEM image illustrates the methodology of surface defect analysis using a 43×34 mesh (1462 squares) to quantify and classify surface irregularities*

Fig. 3 (a) shows SEM image with a superimposed 43×34 grid applied for systematic defect assessment. Fig. 3 (b) shows identification of key surface features, including sharp and smooth surfaces, crack width, pitting density, impurities, and microcracks, marked for comparative evaluation.

Magnification x 100 & Ra < 1.25

Magnification x 100 & Ra < 2.5

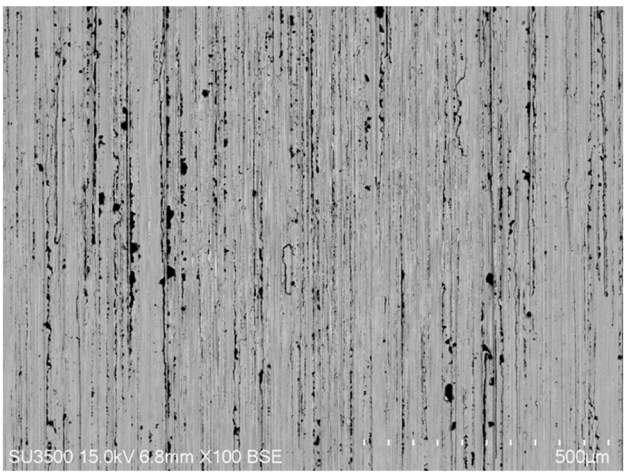

(**a**)

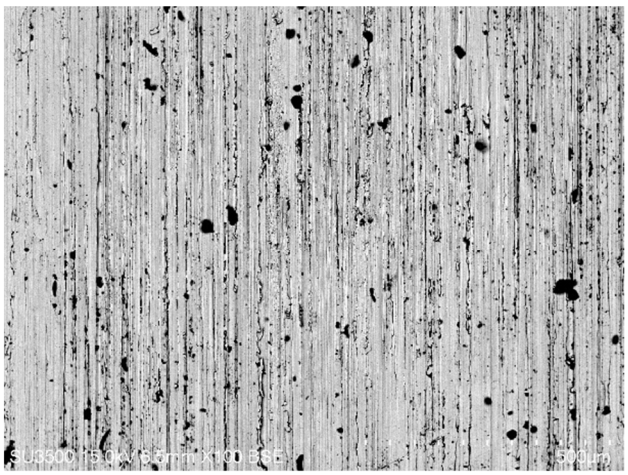

(**b**)

Fig. 4 *Surface images of two samples with roughness values of Ra < 1.25 µm and Ra < 2.5 µm, observed at ×100 magnification*

In the Fig. 4 (a) the first sample (Ra < 1.25 µm) shows a surface with fine, evenly distributed linear scratches and minor irregularities. In the Fig 4 (b) the second sample (Ra < 2.5 µm) exhibits a surface with visible grooves, deeper scratches, and areas of irregular texture.

Tab. 1 *Detailed comparison of surface characteristics of samples with different roughness (Ra<2.5 and Ra<1.25) at ×100 magnification; The analysis includes the proportions of the offenses, the width of the cracks, their frequency, the presence of impurities and the number of spots; The conclusions concern potential applications and effects on tribological properties*

No.	Parameter	Ra < 2.5	Ra < 1.25	Comments
1	Sharp surface features	35% ± 3.5% (approx. 512 grids)	15% ± 1.5% (approx. 219 grids)	Sharp protrusions identified by analyzing the edge shapes in the grids.
2	Smooth surface	65% ± 6.5% (approx. 950 grids)	85% ± 8.5% (approx. 1243 grids)	Smooth protrusions cover all structures with a rounded profile in the mesh analysis.
3	Average crack width (µm)	2.5 ± 0.25	1.8 ± 0.18	The crack width was calculated as an average of 15 measurements in different areas of the mesh.
4	Pitting density (pits/100 grids)	8 ± 0.8 pits/100 grids	3 ± 0.3 pits/100 grids	The number of pits was average based on representative areas.
5	Number of impurities (stains)	12 ± 1.2 (across the grid)	5 ± 0.5 (all over the grid)	Impurities identified from SEM image contrast.
6	Presence of microcracks	Present in 18% ± 1.8% of mesh areas (approx. 263 grids)	Present in 5% ± 0.5% of mesh areas (approx. 73 grids)	Microcracks were determined based on their characteristic geometry and length.
7	Average microcrack length (µm)	4.8 ± 0.48	2.1 ± 0.21	The length was measured on 10 randomly selected cracks on both surfaces.

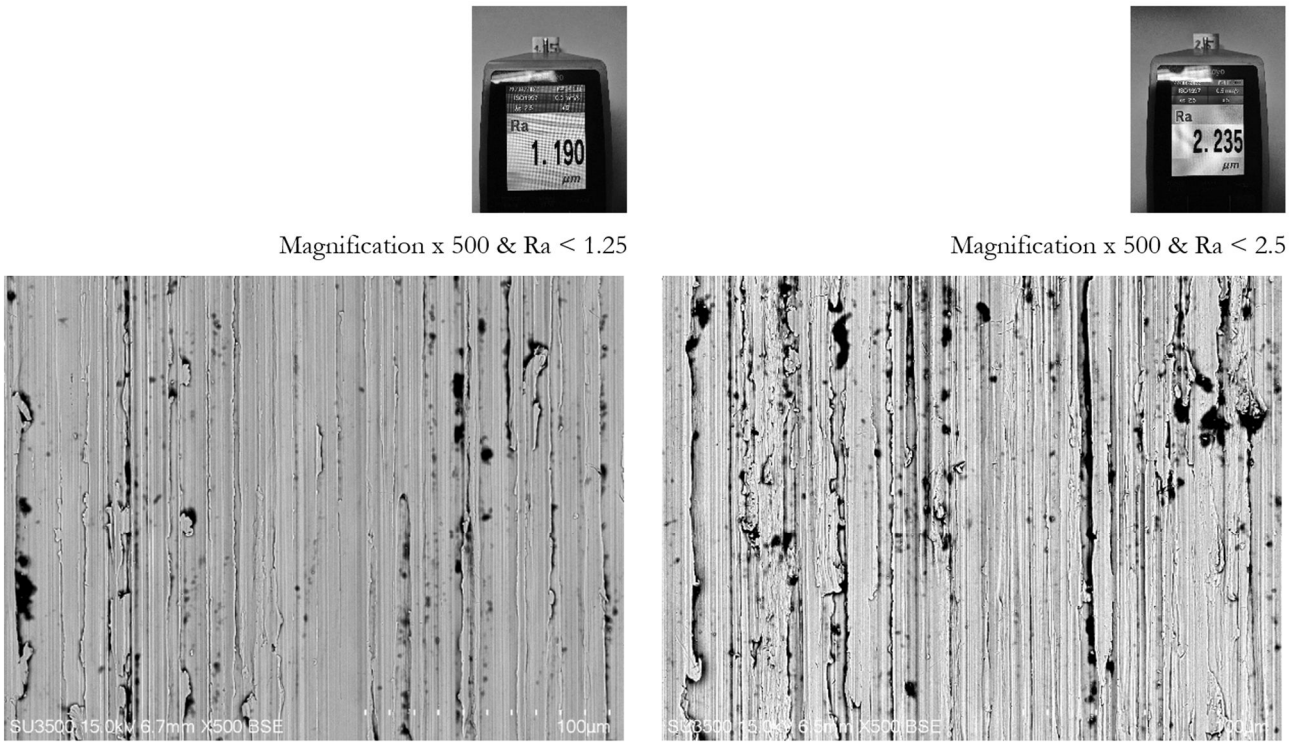

Fig. 5 *Surface images of two samples with roughness values of* Ra *< 1.25 µm and* Ra *< 2.5 µm, observed at ×500 magnification*

In the Fig. 5 (a) the first sample (Ra < 1.25 µm) exhibits a surface with distinct linear scratches, shallow grooves, and occasionally elongated depressions, aligned with the machining direction. In the Fig. 5 (b) the second sample (Ra < 2.5 µm) shows irregularly shaped grooves, deeper pits, and protrusions resembling fractured materiál. Asymmetrical deformations and scattered structures resembling contaminants are also visible.

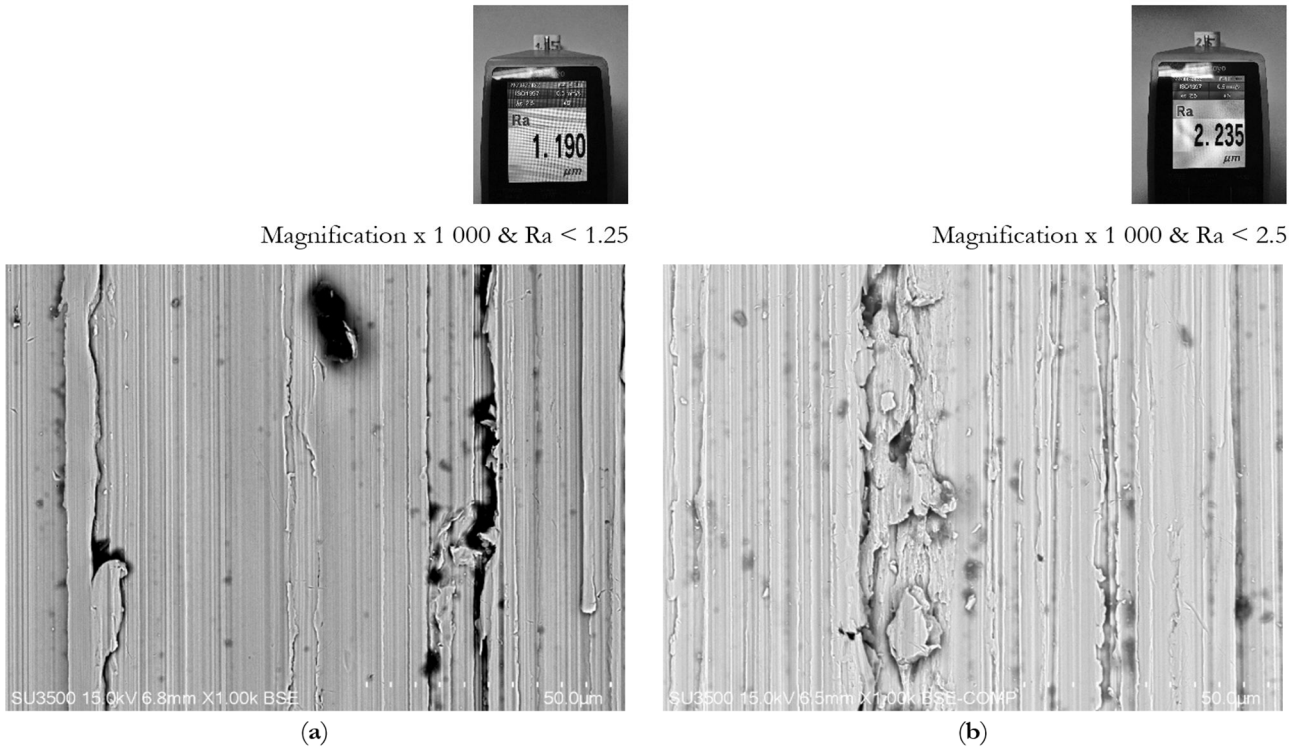

Fig. 6 *Surface images of two samples with roughness values* Ra *< 1.25 µm and* Ra *< 2.5 µm, observed at a magnification of ×1000*

In the Fig. 6 (a) the first specimen (Ra < 1.25 μm) shows a surface with fine, linear scratches, narrow grooves and isolated microcracks, mainly in accordance with the direction of processing. In the Fig. 6 (b) the second sample (Ra < 2.5 μm) shows a surface characterized by irregular grooves, diffuse depressions and micro-cracks of varying width and length, accompanied by impurity-like protrusions and asymmetric surface features.

Tab. 2 *Comparative analysis of the surface characteristics of samples at magnification at x500, considering the percentage of sharp and mild protrusions, the width of cracks, their frequency, and the number of dirt stains; The results indicate the influence of roughness parameters on the quality and tribological properties of the surface*

No.	Parameter	Ra < 2.5	Ra < 1.25	Comments
1	Sharp surface features	45% ± 4.5% (approx. 658 grids)	20% ± 2% (approx. 292 grids)	The Ra < 2.5 μm surfaces exhibit a higher percentage of sharp edges, reflecting the presence of pronounced, angular surface features resulting from rougher machining conditions. In contrast, the Ra < 1.25 μm samples demonstrate smoother transitions and fewer sharp protrusions, indicative of precision machining and reduced mechanical stress.
2	Smooth surface	55% ± 5.5% (approx. 804 grids)	80% ± 8% (approx. 1170 grids)	Mellow performances are dominant in Ra < 1.25 μm surfaces, characterized by rounded edges and smoother microgeometry. These features reduce tribological resistance, enhancing the wear properties of the material. The Ra < 2.5 μm samples, with a lower Smooth surface, display a more uneven surface with increased frictional resistance.
3	Average crack width (μm)	3.2 ± 0.32	2.1 ± 0.21	The wider cracks observed in Ra < 2.5 μm samples suggest that the material underwent greater mechanical stress or deformation during processing. Conversely, the narrower cracks in Ra < 1.25 μm surfaces indicate a more uniform stress distribution and superior structural integrity, which is beneficial for load-bearing applications.
4	Pitting density (pits/100 grids)	12 ± 1.2 pits/100 grids	5 ± 0.5 pits/100 grids	Pitting frequency is significantly higher in Ra < 2.5 μm samples, due to stress concentrations and localized material removal. The lower pitting frequency in Ra < 1.25 μm surfaces reflects a more controlled machining process, where surface defects are minimized, leading to better material performance in corrosive environments.
5	Number of impurities (stains)	25 ± 2.5 (all over the grid)	10 ± 1 (across the grid)	The impurities seen in SEM images manifest as differences in brightness, indicating the presence of sediment or inclusions. Surfaces of Ra < 2.5 μm have more of them, which is due to their greater roughness and ability to retain pollutants. Ra surfaces < 1.25 μm are smoother and cleaner, which promotes better quality components.
6	Presence of microcracks	Present in 22% ± 2.2% of the mesh areas (approx. 322 squares)	Present in 8% ± 0.8% of mesh areas (approx. 117 squares)	Microcracks were determined based on their characteristic geometry.
7	Average microcrack length (μm)	5.3 ± 0.53	2.5 ± 0.25	The length was measured on 15 randomly selected cracks.

Tab. 3 *Comparative analysis of sample surfaces at x1000 magnification, considering the percentage of sharp and mild protrusions, crack width, pitting frequency, and amount of contamination*

No.	Parameter	Ra < 2.5	Ra < 1.25	Comments
1	Sharp surface features	50% ± 5% (approx. 731 grids)	25% ± 2.5% (approx. 366 grids)	The sharp lugs are distinguished by clear edges in the mesh.
2	Smooth surface	50% ± 5% (approx. 731 grids)	75% ± 7.5% (approx. 1096 squares)	The gentle protrusions have a rounded shape and greater regularity.
3	Average crack width (μm)	2.8 ± 0.28	1.9 ± 0.19	The features are narrower and more uniform in Ra < 1.25 samples.
4	Pitting density (pits/100 grids)	15 ± 1.5 pits/100 grids	7 ± 0.7 pits/100 grids	The pitting in the Ra < 2.5 samples is deeper and more irregular in distribution.
5	Number of impurities (stains)	30 ± 3 (across the grid)	12 ± 1.2 (across the grid)	Debris appears as dark, irregular spots visible in the SEM image.
6	Presence of microcracks	Present in 25% ± 2.5% of the mesh areas (approx. 366 squares)	Present in 10% ± 1% of mesh areas (approx. 146 squares)	Microcracks in Ra < 2.5 are more branched.
7	Average microcrack length (μm)	6.5 ± 0.65	3.2 ± 0.32	Microcracks in Ra < 1.25 samples are shorter and straighter.

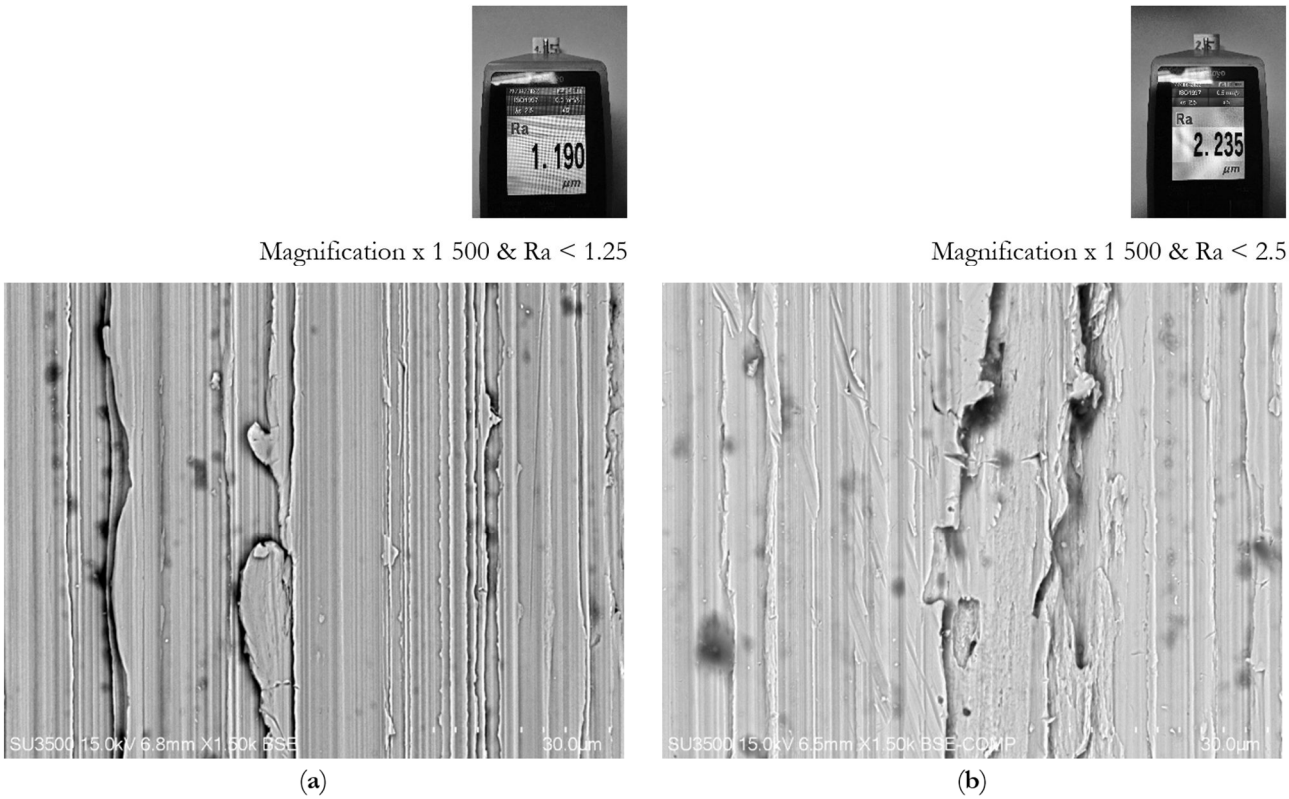

Fig. 7 *Surface images of specimens with roughness values Ra < 1.25 μm and Ra < 2.5 μm, observed at a magnification of ×1500*

In the Fig. 7 (a) the first specimen (Ra < 1.25 μm) shows linear grooves with smooth edges, occasional shallow indentations, and a few microcracks consistent with the direction of processing. In the Fig. 7 (b) the second specimen (Ra < 2.5 μm) exhibits deeper irregularly edged grooves, numerous indentations of different shapes, and a higher density of microcracks with branching patterns.

Tab. 4 *Comparison of surface features at x1500 magnification: detailed analysis of acute and mild offences, pitting, contamination, and their effect on tribological properties*

No.	Parameter	Ra < 2.5	Ra < 1.25	Comments
1	Sharp surface features	40% ± 8% (approx. 585 grids)	20% ± 4% (approx. 293 grids)	The sharp protrusions in Ra < 2.5 are more irregular in shape, often with sharp edges.
2	Smooth surface	60% ± 12% (approx. 877 grids)	80% ± 16% (approx. 1169 squares)	The mellow lugs in Ra < 1.25 are more rounded and evenly distributed.
3	Average crack width (μm)	2.3 ± 0.46	1.5 ± 0.3	The cracks in Ra < 2.5 are wider and more branched compared to Ra < 1.25 samples.
4	Pitting density (pits/100 grids)	12 ± 2.4 pits/100 grids	6 ± 1.2 pits/100 grids	Pitting in Ra < 2.5 is deeper, irregular, and more likely to occur in groups.
5	Number of impurities (stains)	25 ± 5 (across the grid)	10 ± 2 (across the grid)	The impurities in Ra < 2.5 are more diffuse and irregular in shape.
6	Presence of microcracks	Present in 30% ± 6% of mesh areas (approx. 439 grids)	Present in 15% ± 3% of mesh areas (approx. 219 squares)	Microcracks in Ra < 2.5 have an irregular course and a longer length.
7	Average microcrack length (μm)	7.2 ± 1.44	3.6 ± 0.72	The microcracks in Ra < 1.25 are more homogeneous, but much shorter.

Magnification x 2 000 & Ra < 1.25

Magnification x 2 000 & Ra < 2.5

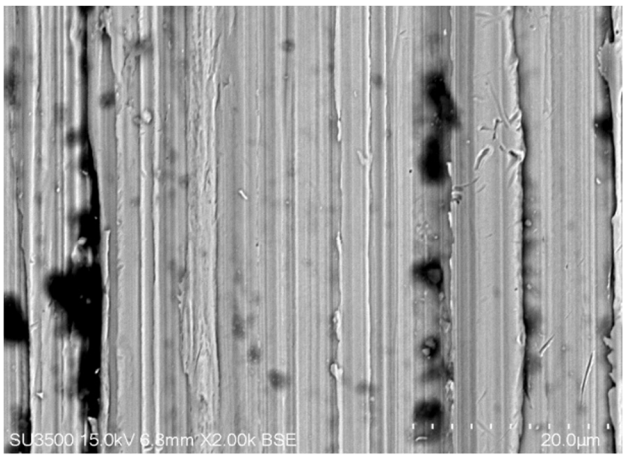

(**a**)

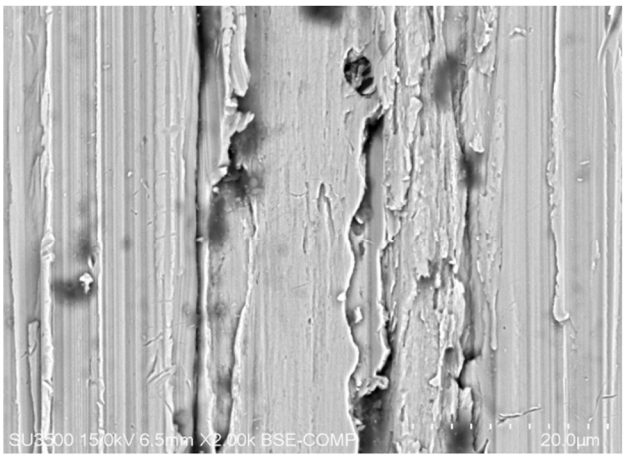

(**b**)

Fig. 8 *Surface images of samples with roughness values Ra < 1.25 μm and Ra < 2.5 μm, observed at ×2000 magnification*

In the Fig. 8 (a) the first sample (Ra < 1.25 μm) shows fine, linear grooves with minimal irregularities, isolated impurities appearing as small dark spots, and shallow microcracks. In the Fig. 8 (b) the second sample (Ra < 2.5 μm) exhibits pronounced grooves with uneven edges, larger clusters of impurities, and widespread microcracks with branching and interconnected patterns.

Tab. 5 *Surface analysis at x2000 magnification: number and characteristics of vices, pits, contaminants, and their impact on the tribological properties of the surface*

No.	Parameter	Ra < 2.5	Ra < 1.25	Comments
1	Sharp surface features	45% ± 9% (approx. 658 grids)	25% ± 5% (approx. 366 grids)	Sharp edges in Ra < 2.5 μm samples are characterized by distinct, angular protrusions with irregular and jagged geometries. These features contribute to increased friction and wear resistance. In Ra < 1.25 μm samples, sharp edges are smoother and less frequent, aligning with a more uniform and controlled machining process.
2	Smooth surface	55% ± 11% (approx. 804 grids)	75% ± 15% (approx. 1096 squares)	Mellow regions dominate Ra < 1.25 μm samples, with smooth, rounded geometries that minimize surface friction and enhance wear resistance. In Ra < 2.5 μm samples, these regions are less prevalent and interrupted by sharper, irregular features, increasing surface roughness and tribological impact.
3	Average crack width (μm)	1.8 ± 0.36	1.2 ± 0.24	Cracks in Ra < 2.5 μm surfaces are wider and show irregular, branching patterns that intersect grooves and pits. In Ra < 1.25 μm surfaces, cracks are narrower, more linear, and align with machining directions, reducing stress concentration, and improving material stability.
4	Pitting density (pits/100 grids)	15 ± 3 pits/100 grids	8 ± 1.6 pits/100 grids	Pits in Ra < 2.5 μm surfaces are larger and irregularly distributed, often associated with areas of high stress or material wear. In Ra < 1.25 μm samples, pits are smaller, more circular, and appear in consistent patterns, reflecting precise machining and better stress management.
5	Number of impurities (stains)	30 ± 6 (across the grid)	12 ± 2.4 (all over the grid)	Impurities in Ra < 2.5 μm surfaces are irregular, forming concentrated clusters around defects such as pits and microcracks. In Ra < 1.25 μm samples, impurities are fewer, smaller, and evenly spaced, which supports higher cleanliness and processing precision.
6	Presence of microcracks	Present in 35% ± 7% of mesh areas (approx. 512 squares)	Present in 20% ± 4% of mesh areas (approx. 293 squares)	Microcracks in Ra < 2.5 μm surfaces are longer, more branched, and frequently connect to pits and grooves, increasing material degradation risk. In Ra < 1.25 μm surfaces, microcracks are shorter, less complex, and more evenly spaced, which reduces the potential for crack propagation.
7	Average microcrack length (μm)	6.5 ± 1.3	3.0 ± 0.6	Longer microcracks in Ra < 2.5 μm surfaces indicate higher material stress and greater susceptibility to mechanical failure. Shorter microcracks in Ra < 1.25 μm surfaces reflect improved structural cohesion and better resistance to stress-induced damage.

Magnification x 2 500 & Ra < 1.25

Magnification x 2 500 & Ra < 2.5

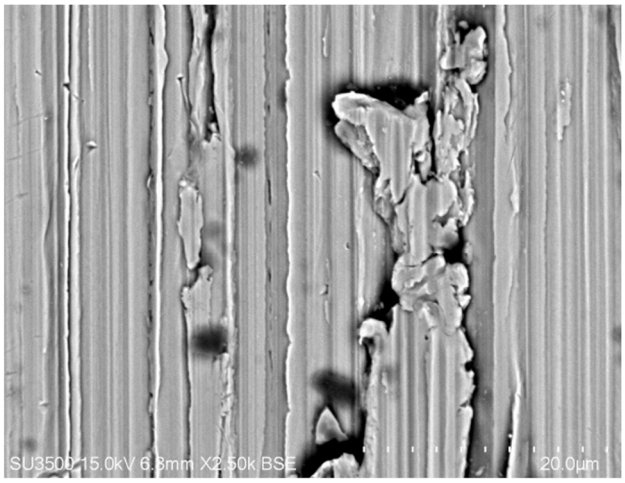

(**a**)

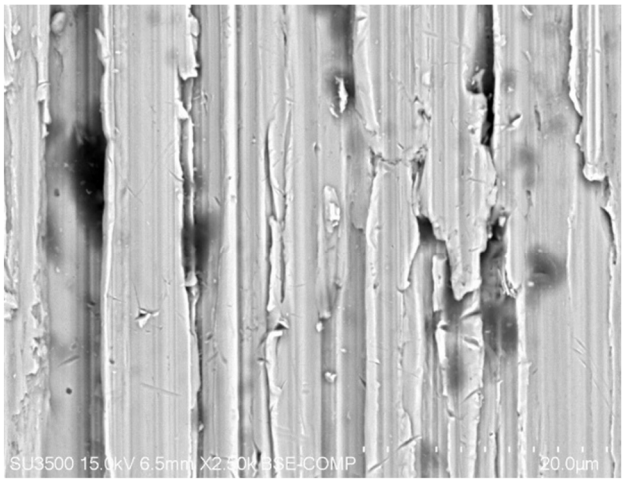

(**b**)

Fig. 9 *Surface images of samples with roughness values Ra < 1.25 μm and Ra < 2.5 μm, observed at ×2500 magnification*

In the Fig. 9 (a) the first sample (Ra < 1.25 μm) shows linear grooves with smooth, well-defined edges. Impurities appear as small, circular, or elongated dark spots, while microcracks are narrow and straight. In the Fig. 9 (b) the second sample (Ra < 2.5 μm) exhibits irregular grooves with jagged edges and deeper profiles. Impurities are larger and clustered, while microcracks show pronounced branching and widening.

Magnification x 2 500 & Ra < 1.25

Magnification x 2 500 & Ra < 2.5

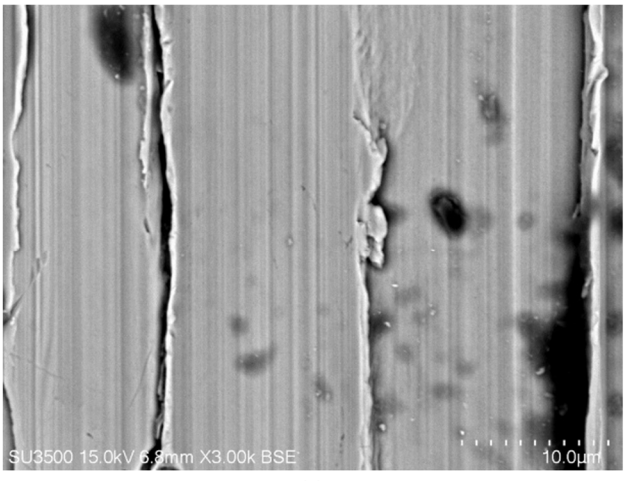

(**a**)

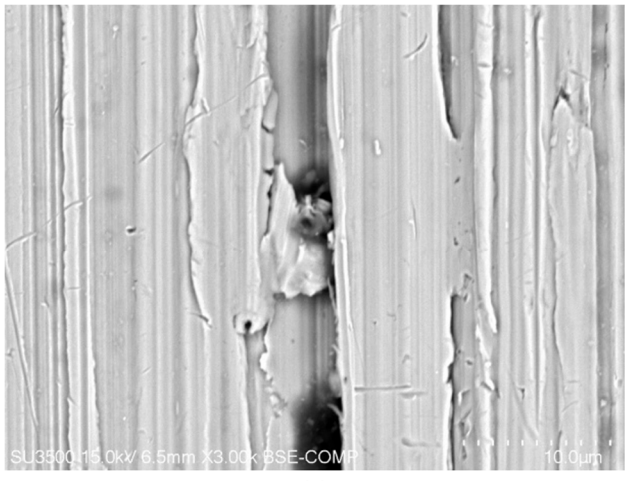

(**b**)

Fig. 10 *Surface images of samples with roughness values Ra < 1.25 μm and Ra < 2.5 μm, observed at ×3000 magnification*

In the Fig. 10 (a) the first sample (Ra < 1.25 μm) shows linear grooves with smooth, continuous edges, interspersed with isolated micro-pits that are circular or slightly elongated. Protrusions are minimal and symmetrical, with contaminants appearing as small, round dark spots. In the Fig. 10 (b) the second sample (Ra < 2.5 μm) exhibits irregular grooves with uneven, jagged edges. Micro-pits are larger and irregularly shaped, with protrusions that appear asymmetrical and more pronounced. Contaminants are more concentrated and form clusters of varying shapes and sizes.

Tab. 6 *Surface analysis at x2500 magnification: number and characteristics of protrusions, pits, contaminants, and their impact on tribological and mechanical properties*

No.	Parameter	Ra < 2.5	Ra < 1.25	Comments
1	Sharp surface features	50% ± 10% (approx. 731 grids)	30% ± 6% (approx. 439 grids)	Sharp edges in Ra < 2.5 μm surfaces dominate irregular areas, with jagged geometries indicating uneven machining and increased stress concentrations. In Ra < 1.25 μm surfaces, sharp features are fewer and smoother, contributing to better surface uniformity and lower friction.
2	Smooth surface	50% ± 10% (approx. 731 grids)	70% ± 14% (approx. 1023 grids)	Mellow protrusions on Ra < 1.25 μm surfaces are smooth, uniform, and dominate the surface microgeometry, enhancing overall consistency. In contrast, Ra < 2.5 μm surfaces exhibit fewer mellow regions, which are often disrupted by sharp features, leading to reduced surface quality.
3	Average crack width (μm)	1.6 ± 0.32	1.1 ± 0.22	Cracks in Ra < 2.5 μm surfaces are wider and more irregular, with branching patterns connected to pits. In Ra < 1.25 μm surfaces, cracks are narrower, more linear, and evenly distributed, reflecting improved structural integrity and reduced material stress.
4	Pitting density (pits/100 grids)	18 ± 3.6 pits/100 grids	10 ± 2 pits/100 grids	Pitting in Ra < 2.5 μm surfaces is irregular and deep, often associated with clusters of impurities. In Ra < 1.25 μm surfaces, pits are smaller, shallower, and more uniform, reducing the likelihood of material degradation.
5	Number of impurities (stains)	35 ± 7 (across the grid)	15 ± 3 (across the grid)	Impurities in Ra < 2.5 μm surfaces are larger and more diffuse, with uneven distribution that may correlate with stress concentrations. In Ra < 1.25 μm surfaces, impurities are smaller, more uniform, and less frequent, indicating better machining cleanliness.
6	Presence of microcracks	Present in 40% ± 8% of mesh areas (approx. 585 squares)	Present in 25% ± 5% of mesh areas (approx. 366 squares)	Microcracks in Ra < 2.5 μm surfaces are longer, more branched, and connected to grooves and pits, increasing the risk of crack propagation. In Ra < 1.25 μm surfaces, microcracks are shorter, straighter, and less frequent, reflecting better resistance to mechanical wear.
7	Average microcrack length (μm)	7.0 ± 1.4	3.5 ± 0.7	Longer microcracks in Ra < 2.5 μm surfaces indicate higher stress and material fatigue. In Ra < 1.25 μm samples, shorter microcracks improve durability and minimize the likelihood of crack growth under load.

Tab. 7 *Surface analysis at x3000 magnification: micro-pitting, number and shape of transgressions, presence of impurities and their impact on durability and tribological properties*

No.	Parameter	Ra < 2.5	Ra < 1.25	Comments
1	Sharp surface features	60% ± 12% (approx. 877 grids)	35% ± 7% (approx. 512 grids)	The sharp features in Ra < 2.5 μm samples are irregular and angular, forming uneven patterns across the surface, often associated with higher stress and material strain. In Ra < 1.25 μm surfaces, the sharp performances are smoother and better aligned, contributing to enhanced surface uniformity and reduced tribological wear.
2	Smooth surface	40% ± 8% (approx. 585 grids)	65% ± 13% (approx. 950 grids)	Mellow features dominate in Ra < 1.25 μm surfaces, appearing as smooth and rounded regions that enhance tribological performance and reduce friction. In Ra < 2.5 μm surfaces, mellow regions are interrupted by sharper elements, creating a rougher surface that can affect wear properties negatively.
3	Average crack width (μm)	1.3 ± 0.26	0.9 ± 0.18	Cracks in Ra < 2.5 μm surfaces are wider, with irregular branching patterns that often intersect pits and grooves, increasing susceptibility to material fatigue. In Ra < 1.25 μm samples, the cracks are narrower and more uniform, reflecting a more controlled stress distribution and better material stability.
4	Pitting density (pits/100 grids)	22 ± 4.4 pits/100 grids	12 ± 2.4 pits/100 grids	Pitting in Ra < 2.5 μm surfaces is deeper and more irregular, with pits clustering in areas of material weakness. In Ra < 1.25 μm surfaces, pits are smaller, shallower, and uniformly distributed, minimizing the risk of surface degradation and improving overall durability.
5	Number of impurities (stains)	40 ± 8 (across the grid)	18 ± 3.6 (all over the grid)	Impurities in Ra < 2.5 μm samples are larger and irregular, often concentrated near grooves and microcracks, indicating less efficient cleaning or machining processes. In Ra < 1.25 μm surfaces, impurities are fewer, more evenly distributed, and smaller in size, pointing to improved surface cleanliness.
6	Presence of microcracks	Present in 45% ± 9% of mesh areas (approx. 658 squares)	Present in 30% ± 6% of mesh areas (approx. 439 grids)	Microcracks in Ra < 2.5 μm surfaces are longer and show complex branching, often connected to pits and sharp features, increasing the risk of crack propagation under stress. In Ra < 1.25 μm surfaces, microcracks are shorter, less branched, and more evenly spaced, providing improved resistance to fatigue and mechanical wear.
7	Average microcrack length (μm)	6.5 ± 1.3	3.0 ± 0.6	The longer microcracks in Ra < 2.5 μm samples indicate higher stress and reduced material durability, posing a greater risk under cyclic loading. In Ra < 1.25 μm surfaces, shorter microcracks reflect improved material cohesion and greater resistance to crack propagation, enhancing overall reliability.

In the studies of the microstructure of the surface layer of samples with different surface roughness (Ra), the SEM technique was used for a detailed analysis of the sur-face morphology. Results answered three key research questions, while revealing some universal surface features and problems regardless of the applied SEM magnification and Ra value.

During the research conducted, changes in surface morphological features de-pending on SEM magnification were analyzed. The results clearly showed that in the samples with roughness Ra < 2.5 and Ra < 1.25, the basic morphological characteristics retain their characteristics regardless of the magnification applied. At all magnifications, from x100 to x3000, irregularities such as sharp and mild protrusions, pitting, microcracks, and debris were observed. Increasing magnification only revealed greater detail of the structure and more precise proportions between individual elements of the microstructure.

For example, the percentage of sharp protrusions in samples with Ra < 2.5 increased from 35% at x100 magnification to 60% at x3000. For Ra < 1.25, these proportions ranged from 15% to 35%, respectively. This means that although the relative values varied, the sharp protrusions themselves were present regardless of magnification. Similarly, mild protrusions in samples with Ra < 1.25 remained dominant at all magnifications, although their proportion decreased from 85% at x100 to 65% at x3000. Thus, surface irregularities, although they differed proportionally, were a constant element of morphology regardless of the scale of observation.

Based on observational and analytical studies, it can be clearly stated that problems resulting from surface irregularities occur regardless of the roughness value Ra. Analysis of samples with Ra < 1.25 revealed that despite reduced roughness and a more regular surface structure, irregularities were still present and could pose potential functional problems. For example, the average crack width in these samples ranged from 0.9 μm to 1.8 μm depending on magnification, and the pitting frequency was as high as 12 per 100 grids at x3000 magnification. In addition, microcracks, although shorter (2.1 μm to 3.6 μm), were still present in 30% of the lattice areas at highest magnification.

This indicates that even at lower roughness, the surface is not perfectly smooth, and the presence of these microstructural irregularities can lead to the initiation of damage, especially in demanding operating environments. Therefore, from the point of view of the designer and user, these tests have shown that regardless of the magnitude of the measured parameters Ra, the problem of stress concentration caused by local irregularities only decreases but is not eliminated in the case of milling machining.

According to the authors of the study, the conducted research allowed us to capture the functional significance of surface unevenness in the context of the selection of roughness parameters at the design stage of responsible machine parts. The increase in SEM magnification from x100 to x3000 allowed for a more precise grasp of the proportions between individual morphological features. For example, the number of impurities in samples with Ra < 2.5 increased from 12 spots on the entire grid at x100 to 40 at x3000, and in samples with Ra < 1.25 – from 5 to 18. At the same time, the microcracks, although shorter at Ra < 1.25, were more pronounced and more visible at higher magnification.

The results of the research presented in this paper show that even at lower values of Ra, inequalities can be a significant problem, because reducing the scale of observations only changes the proportion and distribution of these elements. For example, pit-ting at Ra < 1.25 was more uniform and shallower than at Ra < 2.5, but its presence was constant, indicating that it cannot be ignored when evaluating surface functionality.

The research method presented in the paper, according to its authors, has sufficiently proven that the importance of integrating SEM with profilometry makes engineering sense. Integrating advanced imaging techniques such as SEM with traditional profilometry allows for a more comprehensive understanding of the causes of surface layer unevenness. Although classical methods provide numerical values such as Ra, SEM reveals microstructural details that can affect surface functionality and final decisions on whether to accept or reject the adopted roughness parameters at the design stage of the responsible mechanical parts. This is of key importance for tribological phenomena, because even short discontinuities in the material structure can initiate damage as a result of material fatigue, and irregular protrusions can promote the formation of corrosion centers, and in pneumatic and hydraulic systems cause detachment of microelements, which can contribute to increasing damage to other surfaces or micro-blocking of the responsible control valves.

One of the significant drawbacks of the adopted method of surface assessment is its subjectivity, resulting from manual measurement and comparison of individual elements of the microstructure. Such an approach can led to interpretation errors and evaluative fatigue, which consequently affects the repeatability of results. Nevertheless, even subjective SEM analysis contributes to the development of engineering intuition – a machine designer or technologist remembers characteristic features of surfaces, such as specific shapes, cracks, depressions, scratches or spots. This allows him to consciously select machining parameters and determine its directivity in the construction drawing, which goes beyond the classic methods of surface characterization based on Ra parameters and profilometry.

In the future, measuring devices such as the SEM used in this study (Fig 11) may be equipped with automated surface analysis algorithms, eliminating the

subjective factor and speeding up the evaluation process. Over time, it can be expected that such techniques will become the industry standard, making SEM testing more common in engineering practice. The introduction of artificial intelligence systems for image analysis will allow for automatic detection and classification of defects, increasing the precision and repeatability of results.

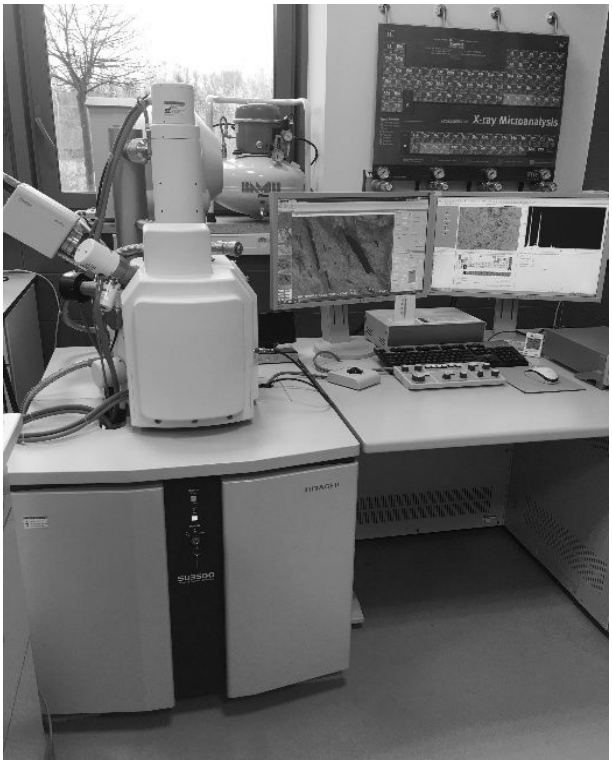

Fig. 11 *Hitachi SU3500 scanning electron microscope used to take surface images in Poznan Science and Technology Park*

In addition, from a mechanical engineering perspective, an important aspect of surface optimization is the avoidance of excessively low roughness in resting and press-fit joints. Excessive smoothing of the surface can lead to increased costs and higher CO2 emissions. Analysis using Sandvik Coromant software showed that the right balance of roughness parameters can optimize both the durability and the mechanical properties of the joints. Therefore, it is important to consider not only the aesthetics and strength of the surface in the design process, but also the functionality in the context of its intended use, as well as the necessary calculations of the carbon footprint. Analysis of the energy intensity of the process showed that the cutting of surfaces with Ra = 1.25 μm and Ra = 2.5 μm differs in terms of energy consumption and CO_2 emissions. The total carbon dioxide emissions for surface treatments with Ra = 1.25 were 35.9 g CO_2, while for Ra = 2.5 it was 34.2 g CO_2, which means a reduction in emissions of about 4.7%. In terms of emission intensity measured in g/kWh, the value was 573 g/kWh for Ra = 1.25 and 546 g/kWh for Ra = 2.5, respectively, representing a difference of 4.7%. On the other hand, the demand for electricity (Work per Component) was 0.0626 kWh for Ra = 1.25 and 0.0622 kWh for Ra = 2.5, which suggests slightly lower energy consumption for surfaces with higher Ra. It is worth noting that despite small percentage differences, on an industrial scale this can lead to energy savings and a reduction in the carbon footprint of the entire production process, therefore, according to the authors of the paper, this publication can facilitate design decisions in construction, technology and metrology.

4 Conclusions

Analysis of the microstructure of the surface layers of samples with different Ra roughness using scanning electron microscopy (SEM) provided key data for a better understanding of the relationship between the Ra value and the actual surface structure. Results clearly showed that while a reduction in Ra leads to greater surface uniformity and regularity, it does not eliminate microcracks, micro pitting or other microstructural defects. These defects can significantly affect the tribological properties and service life of structural elements, which means that the mere fulfillment of the Ra requirement in the technical documentation does not guarantee the absence of surface damage.

Based on the results obtained, the Law of Microstructural Roughness was formulated, which reads: "Microstructural irregularities are inevitable in machining processes, even with a significant reduction in the Ra value. The final quality of the surface layer depends not only on the Ra value, but also on the actual surface microstructure, which should be analysed in a comprehensive manner – using both contact and non-contact methods and microscopic examinations."

Confirmation of this right results not only from the research carried out as part of this work, but also from numerous scientific studies carried out by other research teams. For example, Nagy A. et al. [15] showed that there is a clear relationship between milling parameters and changes in roughness deviation in different directions. Their research showed that the distribution of deviations in roughness profiles at several measurement points can vary, which has a direct impact on the functional properties of the surface.

The law of microstructural roughness has also been confirmed in the research of Wang L. et al. [16], who proved that changes in surface roughness also apply to gray cast iron. In their research, they emphasized the need for experimental optimization of cutting data through appropriate tool selection and wear control, which allows for optimal surface quality. Their results indicate that achieving the required surface roughness should be based on real-world experiments adapted to the machining conditions. A similar approach was proposed by Timárová L. et al. [17], who developed a methodology for planned experiments in the evaluation of Ra parameters, which

allows to increase the accuracy of the obtained results and at the same time reduce the number of required trials.

In addition, studies by Majerík J. et al. [18] on surface topography, roughness and machining accuracy have shown that these parameters are directly related to the chip formation process. Their analysis shows that differences in the Ra value can be due to the type of cutting tool used and the characteristics of the chips generated. The measurement of surface roughness after DNMG and WNMG treatment, despite identical technological conditions, showed differences in Ra values depending on the processed material. This phenomenon has been confirmed by micro geometric studies and observations of the chip formation process, the structure of which has been described in the form of diagrams illustrating their shape and distribution.

The results of the research directly answer the research questions posed below.

- What additional microstructural information can be obtained from SEM compared to traditional profilometric methods? - SEM reveals important microstructural surface features such as microcracks, pitting, sharp and mild protrusions, and contaminants that remain invisible in classic Ra measurements. Visual surface analysis allows you to identify material discontinuities and assess their impact on the functionality of the components, which provides significant support in the quality control process and decision-making about the release of the product for use.
- How do microstructural differences associate with the Ra value affect tribological properties? - A lower Ra value (Ra < 1.25 μm) promotes greater surface uniformity, which improves its tribological properties and increases fatigue resistance. However, microcracks and other structural defects can occur regardless of the Ra value, which means that simply lowering it does not guarantee full-service life. In practice, this means that even if designers specify the value of Ra as a requirement and it is met, it does not guarantee that the surface is free of critical damage.
- Does the integration of SEM with classic roughness measurement methods allow for a better understanding of surface functionality? - Yes, the integration of SEM with profilometric methods allows for a more accurate analysis of microstructural surface discontinuities by evaluating the shape, distribution, and nature of individual defects. This allows for more informed decision-making about the impact of these features on the functionality and durability of the components. SEM also allows for the assessment of the risk of detachment of surface fragments, as well as the impact of pitting, depressions and microcracks on the accelerated degradation of elements. In some cases, you may want to consider using non-destructive testing, such as computed tomography and ultrasonic analysis, to reveal hidden defects that may affect the reliability of components.

The results of the tests showed that the mere indication of the Ra value in the construction documentation is insufficient to ensure the full quality of the surface. Although the Ra value can be as required in both the machining process and in quality testing, this does not automatically mean the absence of microstructural failures. Therefore, the technical documentation should precisely specify not only the value of Ra, but also the measurement method, measurement direction and frequency of control tests to ensure that the surface parameters are compliant with the functional requirements.

Currently, there is no automated method for the quantitative analysis of surface damage, including, min. the number of microcracks and their relationship to the classification of surface topography. In the present study, this process was carried out manually, which is associated with the risk of subjective interpretations and limited reproducibility of results. It can be assumed that the dynamic development of artificial intelligence systems and image processing algorithms soon will enable automatic detection and classification of defects, which will significantly increase the precision and reliability of surface quality assessments.

In conclusion, this paper describes a methodology that can be widely used in structural design, optimization of machining processes and surface quality control. Conscious determination of roughness parameters in technical drawings and their correct interpretation are crucial for precise design and increasing the durability of engineering components.

References

[1] NOWAKOWSKI, Ł., MIKO, E. (2015). Modele do prognozowania parametru chropowatości Ra powierzchni frezowanych. *Mechanik*, 88. DOI: 10.17814/mechanik.2015.8-9.414.

[2] BUJ-CORRAL, I., SÁNCHEZ-CASAS, X., LUIS-PÉREZ, C. J. (2021). Analysis of AM parameters on surface roughness obtained in PLA parts printed with FFF technology. *Polymers*, 13,

2384. https://doi.org/10.3390/polym13142384.

[3] ABELLÁN-NEBOT, J. V., VILA PASTOR, C., SILLER, H. R. (2024). A review of the factors influencing surface roughness in machining and their impact on sustainability. *Sustainability*, 16, 1917. https://doi.org/10.3390/su16051917.

[4] MOHAMMED, A., ABDULLAH, A. (2018, November). Scanning electron microscopy (SEM): A review. In Proceedings of the 2018 International *Conference* on Hydraulics and Pneumatics—HERVEX, Băile Govora, Romania (Vol. 2018, pp. 7-9). ISSN 1454-8003.

[5] CAZAUX, J. (2005). Recent developments and new strategies in scanning electron microscopy. *Journal of Microscopy,* 217(1), 16-35. https://doi.org/10.1111/j.0022-2720.2005.01414.x.

[6] SZYMAŃSKI, M., PRZESTACKI, D., SZYMAŃSKI, P. (2023). The influence of selected laser engraving parameters on surface conditions of hybrid metal matrix composites. *Materials*, 16, 6575. https://doi.org/10.3390/ma16196575.

[7] RAMEZANI, M., MOHD RIPIN, Z., PASANG, T., JIANG, C. P. (2023). Surface engineering of metals: techniques, characterizations and applications. *Metals*, 13, 1299. https://doi.org/10.3390/met13071299.

[8] SHARMA, S., DWIVEDI, S. P., LI, C., AWWAD, F. A., KHAN, M. I., ISMAIL, E. A. (2024). Unveiling of grain structure, porosity, phase distributions, microstructural morphology, surface hardness, and tribo-corrosion characteristics of nickel and titanium dioxide-based SS-304 steel microwave composite coatings cladding. *Journal of Materials Research and Technology,* 28, 4299–4316. https://doi.org/10.1016/j.jmrt.2024.10.052.

[9] SANGEETHA, M., VASANTHAPRABHU, A., SIVAPRAKASAM, K., NITHYA, S., DHINAKARAN, V., GUNASEKAR, P. (2023). Surface roughness analysis for newly prepared CNT-coated metal matrix: RSM approach. *Applied Nanoscience*, 13, 693–705. https://doi.org/10.1007/s13204-023-02712-y.

[10] LEKSYCKI, K., FELDSHTEIN, E., MARUDA, R. W., KHANNA, N., KRÓLCZYK, G. M., PRUNCU, C. I. (2022). An insight into the effect surface morphology, processing, and lubricating conditions on tribological properties of Ti6Al4V and UHMWPE pairs. *Tribology International*, 170, 107504. https://doi.org/10.1016/j.triboint.2022.107504.

[11] GUPTA, M. K., ETRI, H. E., KORKMAZ, M. E., ROSS, N. S., KRÓLCZYK, G. M., GAWLIK, J., PIMENOV, D. Y. (2022). Tribological and surface morphological characteristics of titanium alloys: A review. A*rchives of Civil and Mechanical Engineering*, 22, 72. https://doi.org/10.1007/s43452-021-00336-8.

[12] WU, B., IBRAHIM, M. Z., RAJA, S., YUSOF, F., MUHAMAD, M. R. B., HUANG, R., KAMANGAR, S. (2022). The influence of reinforcement particles friction stir processing on microstructure, mechanical properties, tribological and corrosion behaviours: a review. *Journal of Materials Research and Technology*, 20, 1940–1975. https://doi.org/10.1016/j.jmrt.2022.05.055.

[13] WANG, R., WANG, B., BARBER, G. C., GU, J., SCHALL, J. D. (2019). Models for prediction of surface roughness in a face milling process using triangular inserts. *Lubricants*, 7(1), 9. https://doi.org/10.3390/lubricants7010009.

[14] YANG, H., ZHENG, H., ZHANG, T. (2024). A review of artificial intelligent methods for machined surface roughness prediction. *Tribology International*, 109935. https://doi.org/10.1016/j.triboint.2023.109935.

[15] NAGY, A., KUNDRÁK, J. (2024). Roughness of face-milled surface topography in directions relative to the feed movement. *Manufacturing Technology*, 24(2), 241-245. https://doi.org/10.21062/mft.2024.024

[16] WANG, L., HAN, L., HE, L., WANG, K., ZHU, X. (2024). Study on the mechanism of improving surface roughness of gray cast iron machining by wiper inserts. *Manufacturing Technology*, 24(3), 478-480. https://doi.org/10.21062/mft.2024.049

[17] TIMÁROVÁ, E., BREZNICKÁ, A., KOPILÁKOVÁ, B. (2023). Application of the method of planned experiment for the evaluation of the surface roughness parameter Ra. *Manufacturing Technology*, 23(3), 348-349. https://doi.org/10.21062/mft.2023.043

[18] MAJERÍK, J., MAJERSKÝ, J., BARÉNYI, I., CHOCHLÍKOVÁ, H., ESCHEROVÁ, J., KUBASÁKOVÁ, M. (2023). Surface roughness, topography, accuracy, chip formation analysis & investigation of M390 and M398 steels after hard machining. *Manufacturing Technology*, 23(1), 60-62. https://doi.org/10.21062/mft.2023.015